Supporting Information for the Manuscript "Helium Droplet-Mediated Deposition and Aggregation of Nanoscale Silver Clusters on Carbon Surfaces"

Ricardo Fernández-Perea,[†] Luis F. Gómez,[‡,⊥] Carlos Cabrillo,[†] Marti Pi,[¶] Alexander O. Mitrushchenkov,[§] Andrey F. Vilesov,[*,‡] and María Pilar de Lara-Castells[*,‖]

[†]*Instituto de Estructura de la Materia (C.S.I.C.), Serrano 123, E-28006, Madrid, Spain*

[‡]*Department of Chemistry, University of Southern California, Los Angeles, California 90089, United States*

[¶]*Department ECM, Facultat de Física, and IN^{2}UB, Universitat de Barcelona, Diagonal 645, E-08028, Barcelona, Spain*

[§]*Université Paris-Est, Laboratoire Modélisation et Simulation Multi Echelle, MSME UMR 8208 CNRS, 5 bd Descartes, 77454 Marne-la-Vallée, France*

[‖]*Instituto de Física Fundamental (C.S.I.C.), Serrano 123, E-28006, Madrid, Spain*

[⊥]*Present Address: IPG Photonics, 3939 Freesom Circle, Str. 130, Santa Clara, CA 95054*

E-mail: vilesov@usc.edu; Pilar.deLara.Castells@csic.es

This Supporting Information provides details of the pairwise potential models used in this work including three tables with the parameters of the different pair interactions as well as a simplified model of the dynamics of an incoming particle interacting with an absorptive surface.

S1 *Ab initio*-Assisted Determination of the $(Ag)_N$/Carbon-Surface Interaction

In this work, the interaction of $(Ag)_N$ clusters with carbon surfaces is described using an additive pairwise potential (PPM) model for both dispersionless and dispersion energy components of the interaction. This PPM model can be viewed as a simplified version of that developed to describe the interaction of helium and molecular nitrogen clusters with carbon nanotubes.[1] The dispersion energy for the Ag−C pair is defined using the D_{as} function of Szalewicz and collaborators,[2–4]

$$E_{\rm int}^{\rm disp}(R_{\rm Ag-C}) = -\sum_{n=6,8} \frac{C_n^{\rm Ag-C}}{R_{\rm Ag-C}^n} f_n\left(\beta^{\rm Ag-C} R_{\rm Ag-C}\right), \tag{S1}$$

where $R_{\rm Ag-C}$ denotes the distance between one Ag atom from the silver nanocluster and one carbon atom of the surface, with the terms f_n $(n = 6, 8)$ standing for the damping functions of Tang and Toennies.[5] The model parameters were extracted from the dispersion energies calculated at coupled-cluster single and doubles and perturbative triples [CCSD(T)] level through the application of the method of increments to the Ag_2/coronene complex (see Ref. 6 for the details). As analyzed in Ref. 6 (see also Ref. 1), the dispersionless interaction is repulsive and grows exponentially as the adsorbate/surface distance decreases. The particular case of the pair Ag−C interaction can be well fitted to the function

$$E_{\rm int}^{\rm disp-less}(R_{\rm Ag-C}) = A\,\frac{e^{(-\alpha\,R_{\rm Ag-C})}}{R_{\rm Ag-C}^{\gamma}}, \tag{S2}$$

where the parameters A, α and γ were derived by fitting the dispersionless interaction energies of the Ag_2/graphene system.[6] These interaction energy contributions were calculated using the dispersionless density functional dlDF of Pernal et al.[2] In its turn, the adequacy of the dlDF scheme was tested againts the benchmarking at CCSD(T) level for the Ag_2/benzene complex.[6] The values of the derived model parameters are collected in Table S1.

Table S1: Parameters defining the dispersionless and dispersion energy contributions to the interaction energy between one Ag atom from a silver cluster and one surface carbon atom.

Atomic Pair	Parameters for the dispersionless pair interaction energy		
	A / eV	α / Å^{-1}	γ
C−Ag	1028.105	1.004	2.145
	Parameters for the dispersion pair interaction energy		
	C_6 / eV·Å^6	C_8 / eV·Å^8	β / Å^{-1}
C−Ag	54.102	348.095	2.754

S2 Determination of Lennard-Jones Pair He−C and Effective He−He Interaction Potentials

The interaction of the helium droplets with surface carbon atoms was represented as a sum of He−C Lennard-Jones 6−12 (LJ) interaction potentials,

$$E_{\rm int}^{\rm LJ}(R_{\rm He-C}) = 4\epsilon \left[\left(\frac{\sigma}{R_{\rm He-C}} \right)^{12} - \left(\frac{\sigma}{R_{\rm He-C}} \right)^{6} \right] \tag{S3}$$

The LJ parameters ϵ (well-depth) and σ (hard core radius) were extracted from *ab initio* calculations for the He/graphene interaction considering three different adsorption sites.[7,8] These *ab initio* calculations were performed by applying the dlDF+D$^*_{as}$ scheme.[7] This is a combined post-Hartree-Fock/DFT scheme where the sum of HF and *intramonomer* correlation contributions is approximated by that obtained through dlDF calculations on periodic surface models.[7] Next, 2- and 3-body *intermonomer* correlation contributions are calculated at CCSD(T) level via the application of the method of increments on surface cluster models, allowing the D$_{as}$ function parametrization (the so-named incremental D$^*_{as}$ parametrization). As described in Ref. 8, the accuracy of this scheme has been assessed by calculating the energies of the low-lying nuclear bound states supported by the laterally averaged ^{4}He/graphite

potentials and comparing them with the best experimental-based estimations. The absolute (relative) deviations from these estimations were less than 0.5 meV (1.5%).[8] The derived LJ parameters along with those obtained for the effective He-He interaction are collected in Table S2.

Table S2: Interaction LJ parameters for helium droplets interacting with carbon surfaces, represented as a sum of LJ He−C interaction potentials, and the effective He-He interaction. For comparison purposes, standard values of the original He-He potential are also shown.

Atomic Pair	σ / Å	ϵ / meV
He−C	3.1169	1.1537
He−He	3.5727	0.1909
He−He	(2.556)	(0.881)

As discussed in the main text, the effective He-He interaction was calculated by following the scheme of Halberstadt and collaborators to study the nuclear dynamics of relatively large helium droplets[9] (see also Refs. 10,11 for similar schemes applied to quantum crystals and neon clusters). The strategy basically consists in replacing helium atoms by fixed-width wave functions ϕ_n centered on each atom, and then classically simulate the time evolution of these centers. Importantly, as stated in Ref. 9 "This is equivalent to classically propagating the helium atoms in an effective interaction potential which is the original He-He interaction potential averaged over the helium wave functions."[9–11] In this work, we have carried out atomistic molecular dynamics simulations using an slightly modified version of the effective He-He interaction potential of Ref. 9. First, LJ parameters were calculated so that our effective LJ-type potential had the same well-depth and equilibrium distance of the effective He-He potential reported in Ref. 9 (1.54 cm^{-1} and 4.20 Å, respectively). This effective LJ-type potential for the He-He interaction resulted in helium droplets with a density 16% below the experimental value for bulk liquid helium at $T = 0.4$ K zero pressure ($\rho = 0.021837$ $\mathring{A}^{-3}$

from Table 2.1 of Ref. 12). Hence, as a second step, the σ parameter was modified until getting the density of bulk liquid for the helium drop. Using the resulting LJ-type potential (see S2), we assessed that the doped helium droplets $Ag_{5000}@He_N$ kept a liquid behaviour until the end of the simulation, with $N = 10000$ and 100000. In particular, it was checked that the density in the bulk of the doped helium droplets had the right value ($\rho = 0.021837$ $\mathring{A}^{-3}$).

As can be seen in Table S2, the well-depth of the effective He-He potential (0.1909 meV) is much smaller than the standard value from the LJ-type He-He potential (0.881 meV). This shift in the well-depth accounts semiquantitatively for the zero-point energy in the system. It is well-known that the zero-point energy of the $^4He_2$ dimer is extremelly large as compared with the well-depth. Thus, the energy of the single $^4He_2$ nuclear bound-state is about -0.000138 meV only.[1] The equilibrium distance of the effective potential (~ 4.01 Å) is much larger than that of the original LJ-type potential (~ 2.87 Å). As mentioned above, the scheme is equivalent to replace each particle by a fixed-width wave-functions ϕ_n centered at its classical position. This is translated in larger mean He-He distances, thus accounting partly for zero point and nuclear delocalization effects in the quantum motion of helium drops.

S3 Interaction of Ag_N Clusters with Helium Droplets

The interaction of Ag_N clusters with the ^4He droplets is expressed as a sum of Ag−He interaction potentials, using the interaction energies calculated at coupled-cluster single and doubles and triples (CCSDT) level by Cargnoni et al.[13] These interaction energies have been fitted to the following function

$$E_{\rm int}(R_{\rm Ag-He}) = Ae^{-\alpha R_{\rm Ag-He}-\beta R^2_{\rm Ag-He}} - F(R_{\rm Ag-He}) \times \left(\frac{C_6}{R^6_{\rm Ag-He}} + \frac{C_8}{R^8_{\rm Ag-He}} + \frac{C_{10}}{R^{10}_{\rm Ag-He}} + \frac{C_{12}}{R^{12}_{\rm Ag-He}} \right),$$

where

$$F(R_{\mathrm{Ag-He}}) = \begin{cases} e^{-(1-D/r)^2} & \text{if} \quad r < D \\ 1 & \text{if} \quad r \geq D, \end{cases} \tag{S4}$$

with the parameters given in Table S3.

Table S3: Parameters of the fit to the Ag-He interaction potential.

Parameters of the pair Ag-He interaction potential	
A / meV	6.7854
α / Å^{-1}	0.6530
β / Å^{-2}	0.3637
D / Å	12.03
C_6 / eV·Å^6	11.8093
C_8 / eV·Å^8	16.3199
C_{10} / eV·Å^{10}	9596.0715
C_{12} / eV·Å^{12}	0.1014×10^{-3}

S4 Desorption in Central Secondary Impacts of Bare Particles

Figure S1 illustrates the case of a secondary impact of a bare Ag_{5000} cluster onto a deposited one (see also movie S6 in Supporting Information) when at the initial position the center-of-mass of both nanoparticles are vertically aligned. At 77 ps the merged particle has already escaped the adsorption potential of the aC surface. In the Helium mediated case, however, the He droplet dynamics inhibit such a possibility. We have performed an additional analysis by displacing the initial center-of-mass lateral position of the incoming cluster. If the center-of-mass positions of deposited and incoming clusters are separated by 12 Å the merged nanoparticles still escape from the surface. In contrast, for a separation of 13 Å the merged nanoparticles stay adsorbed on the surface. Since the estimated diameter of both particles

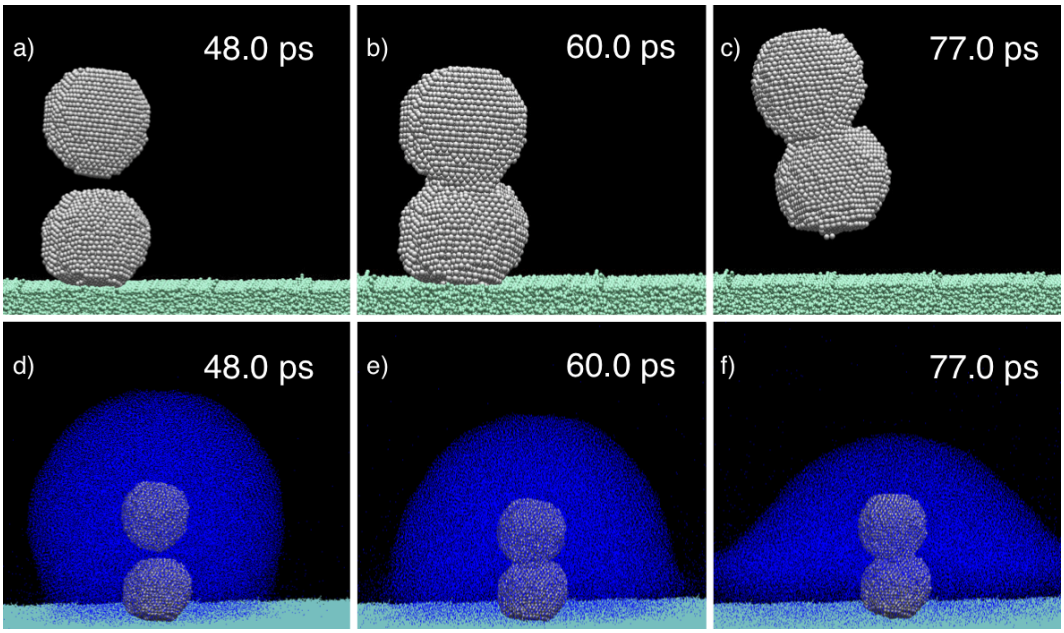

Figure S1: The upper panels illustrate the evolution of a bare central secondary impact of two Ag_{5000} clusters. The lower panels show the evolution when the same impact is mediated by a $^4He_{100000}$ droplet.

is 50 Å the probability of the desorption process ranges from 5.8 to 6.8%, provided that the incoming particle hits to the deposited particle. It is, therefore, not only irrelevant for the He-mediated deposition experiments but quite a marginal effect in general, difficult to be confirmed experimentally. In any case, the result is rather counterintuitive and it deserves some clarification. The key point is that the substrate material must admit elastic vertical deformation at the impact point. Not all the energy should be dissipated in plastic deformation or in incoherent phonon excitations (heat). In order to help in understanding its origin we have developed a simple model of deposition onto an adsorptive surface.

We will consider point-like particles of mass m_p interacting with a surface through a Lennard-Jones potential defined as,

$$V_{\rm ads}^{\rm LJ}(z) = 4\epsilon \left[\left(\frac{\sigma}{z}\right)^{12} - \left(\frac{\sigma}{z}\right)^{6} \right] \tag{S5}$$

where z is the vertical distance from the particle to the surface. The dynamical response of

the surface to the interaction is limited to one vertical damped harmonic vibrational mode characterized by a proper frequency ω_s, an effective mass m_s, and a dampening constant γ_s. The response of the surface is not perturbed by the incoming particles so that ω_s, m_s and γ_s are determined by the characteristics of the surface material. In other words, we have reduced the dynamical response of the surface to just an elastic vertical deformation at the impact point within the harmonic approximation. The corresponding evolution equations reads,

$$\begin{aligned} m_p\,\ddot{z_p} &= -\left.\frac{\mathrm{d}V_{\mathrm{ads}}^{\mathrm{LJ}}(z)}{\mathrm{d}z}\right|_{z\,=\,z_p-z_s} \\ m_s\,\ddot{z_s} &= -m_s\,\omega_s^2 + \left.\frac{\mathrm{d}V_{\mathrm{ads}}^{\mathrm{LJ}}(z)}{\mathrm{d}z}\right|_{z\,=\,z_p-z_s} - \gamma_s\dot{z_s}\ , \end{aligned}$$

where z_p and z_s are respectively the heights of the particle and surface in the laboratory inertial reference frame. The height origin corresponds to the equilibrium position of the surface in the absence of any interaction with the incoming particle. See the left inset in the upper panel of Fig. S2 for an sketch of the model. Within this model dissipation is explicitly taking into the account only through the damping of the surface mode. As shown below, dissipation due to plastic deformation will be considered through adequate initial conditions. The system can be viewed as a Lennard-Jones non-harmonic "oscillator" coupled to the surface harmonic mode. The coupling is determined by the ratio $g = \epsilon/m_s$. In the following, the evolution equations are numerically solved using the Mathematica program checking that the accuracy is enough for the corresponding time window. During all the calculations $\omega_s = 1$ while m_p is fixed to 1 or 2 as appropiate. As a first test, we have checked that decoupling the surface mode ($g \approx 0$)., i.e, in the limit of a rigid surface, and incoming particle rebounds conservatively.

To include the effect of energy dissipation during the plastic deformation of the nanoparticles we rely in the appropriate initial conditions. When a nanoparticle approaches the surface eventually it will begin to both deform itself and to push the surface down. At the

time that the carbon surface at the impact point reaches its maximum downwards elongation, the plastic deformation is also maximum and the velocity is zero. In terms of our simple model, the surface mode is at zero velocity at a downwards position so that the surface mode potential energy equals the part of the initial energy not dissipated as plastic deformation and heat during the impact process. Essentially the same happens in the case of a secondary impact, but now the plastic deformation includes the merging of the impinging particle with an already deformed one at rest onto the surface. Modelling one case or the other from the time of maximum elongation onwards is just a matter of setting $m_p = 1$ or $m_p = 2$. Given that the velocity far from the surface is the same, the initial energy in the simulations, K, is equal in both cases. Let as first assume that also the fraction ΔK giving rise to the elastic deformation of the carbon surface is the same. This determines the initial position of the surface mode coordinate of our model in terms of ΔK for the solution of the evolution equations. As for the particles, we will fix they initial distance to the surface to 1.01σ. The initial velocities are all zero. We fix the parameters of the system to $\sigma = 1.75$, $\epsilon = 0.75$, $m_s = 7.5$, $\gamma_s/m_s = 1.5$ and $\Delta K = 100$. Notice that $g = 0.1 < 1$ and, hence, we are in a weak coupling regime as expected for a surface rigid enough to induce significant nanoparticle plastic deformation. The results are summarized in Fig. S2. The particle of mass 2 desorbs while that of mass 1 remains adsorbed (see upper panel). Reassuringly, with the chosen parameters, the velocity evolution of the $m_p = 1$ case resembles that of bare single Ag_{5000} simulation quite nicely (see the lower panel in Fig. S2 and compare with Figure 5 in the main text). The role of dissipation is essential so that the surface mode needs to be heavily damped (see the right inset in the upper panel of Fig. S2). Otherwise, both particles rebound. The parameters do not need to be accurately tuned to observe the desorption effect. In particular, there is plenty of flexibility in the initial distance of the particles to the surface, neither need to be both the same. More relevantly, ΔK does not need to be equal. Halving ΔK for the mass 2 particle, the desorption still persists (see the inset in the lower panel). Not surprisingly, the maximum velocities depart more than in the case of equal ΔK.

As a matter of fact, below half the energy, we have never observed desorption of the mass 2 particle. Essentially, what happens is that the maximum velocity reached by the particles is determined by the almost unperturbed elastic response of the surface at the impact point. At such a moment, the double mass of the merged particle implies an excess kinetic energy enough to scape from the adsorption potential well.

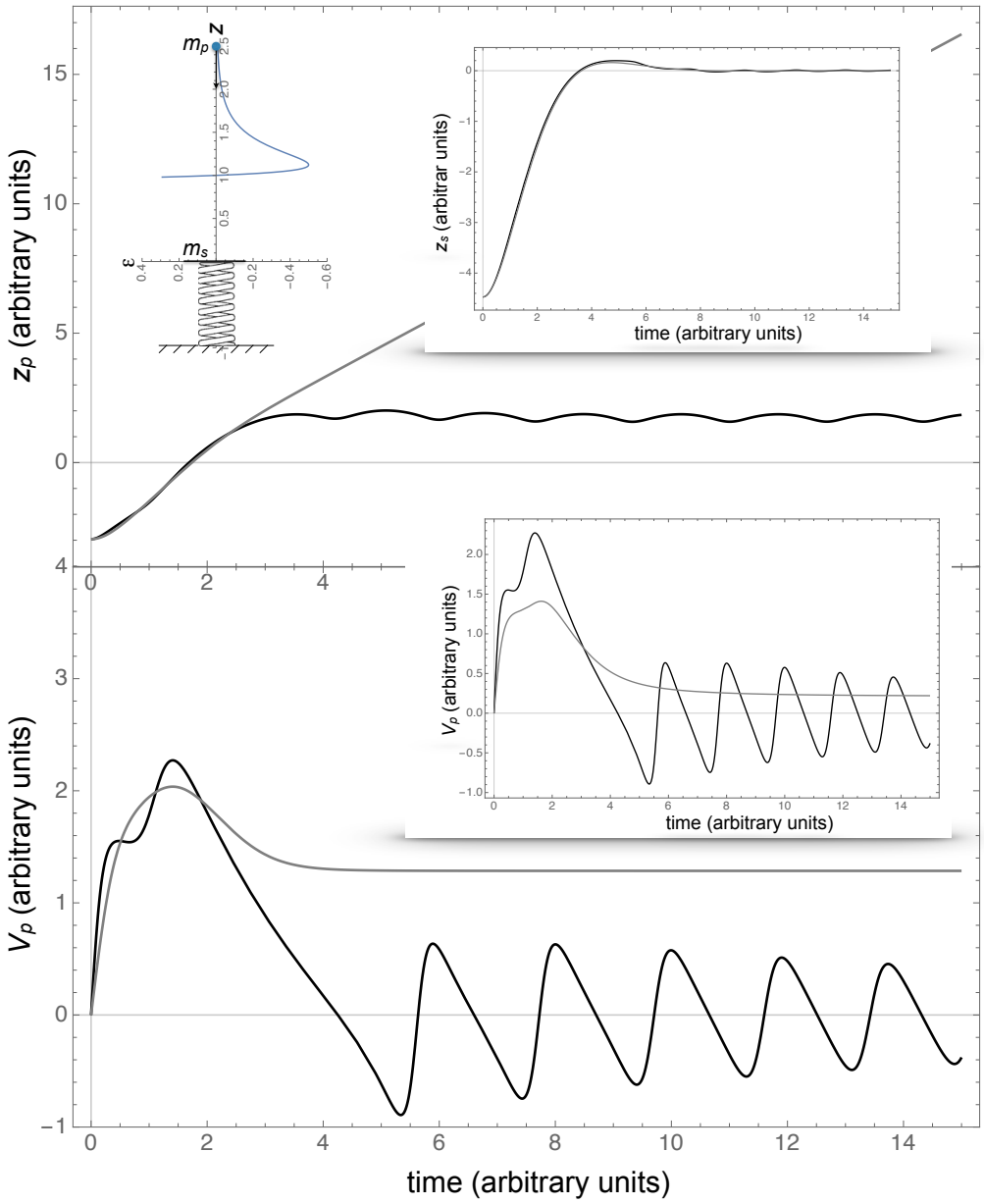

Figure S2: The upper panel shows the evolution of the height of an incoming particle of mass 1 (black curve) and of mass 2 (gray curve). System parameters and initial conditions as explained in the text. The left inset in this panel illustrates de model while the inset in the right display the evolution of the surface position. The lower panel shows the evolution of the particles velocities. The inset in the lower panel corresponds to a ΔK of the mass 2 particle halved.

References

(1) Hauser, A. W.; Mitrushchenkov, A. O.; de Lara-Castells, M. P. Quantum Nuclear Motion of Helium and Molecular Nitrogen Clusters in Carbon Nanotubes. *J. Phys. Chem. C* **2017**, *121*, 3807–3821.

(2) Pernal, K.; Podeszwa, R.; Patkowski, K.; Szalewicz, K. Dispersionless Density Functional Theory. *Phys. Rev. Lett.* **2009**, *103*, 263201.

(3) Podeszwa, R.; Szalewicz, K. Density Functional Theory Overcomes the Failure of Predicting Intermolecular Interaction Energies. *J. Chem. Phys.* **2012**, *136*, 161102.

(4) Podeszwa, R.; Pernal, K.; Patkowski, K.; Szalewicz, K. Extension of the Hartree-Fock Plus Dispersion Method by First-Order Correlation Effects. *J. Phys. Chem. Lett.* **2010**, *1*, 550–555.

(5) Tang, K. T.; Toennies, J. P. An Improved Simple-Model for the van der Waals Potential Based on Universal Damping Functions for the Dispersion Coefficients. *J. Chem. Phys.* **1984**, *80*, 3726–3741.

(6) de Lara-Castells, M. P.; Mitrushchenkov, A. O.; Stoll, H. Combining Density Functional and Incremental Post-Hartree-Fock Approaches for van der Waals Dominated Adsorbate-Surface Interactions: Ag_2/Graphene. *J. Chem. Phys.* **2015**, *143*, 102804.

(7) de Lara-Castells, M. P.; Stoll, H.; Civalleri, B.; Causà, M.; Voloshina, E.; Mitrushchenkov, A. O.; Pi, M. Communication: A Combined Periodic Density Functional and Incremental Wave-Function-Based Approach for the Dispersion-Accounting Time-Resolved Dynamics of ^{4}He Nanodroplets on Surfaces: ^{4}He/Graphene. *J. Chem. Phys.* **2014**, *141*, 151102.

(8) de Lara-Castells, M. P.; Bartolomei, M.; Mitrushchenkov, A. O.; Stoll, H. Transferability and Accuracy by Combining Dispersionless Density Functional and Incremental

Post-Hartree-Fock Theories: Noble gases Adsorption on Coronene/Graphene/Graphite Surfaces. *J. Chem. Phys.* **2015**, *143*, 194701.

(9) Bonhommeau, D.; Lake Jr., P. T.; Quiniou, C. L.; Lewerenz, M.; Halberstadt, N. Modeling the Fragmentation Dynamics of Ionic Clusters Inside Helium Nanodroplets: The Case of $He_{100}Ne_4^+$. *J. Chem. Phys.* **2007**, *126*, 051104.

(10) Sterling, M.; Li, Z.; Apkarian, V. A. Simulations of Quantum Crystals by Classical Dynamics. *J. Chem. Phys.* **1995**, *103*, 5679–5683.

(11) Slavicek, P.; Jungwirth, P.; Lewerenz, M.; Nahler, N. H.; Farnik, M.; Buck, U. Pickup and Photodissociation of Hydrogen Halides in Floppy Neon Clusters. *J. Phys. Chem. A* **2003**, *107*, 7743–7754.

(12) Donnelly, R. J.; Barenghi, C. F. The Observed Properties of Liquid Helium at the Saturated Vapor Pressure. *J. Phys. Chem Ref. Data* **1998**, *27*, 1217–1274.

(13) Cargnoni, F.; Kuś, T.; Mella, M.; Bartlett, R. J. Ground State Potential Energy Surfaces and Bound States of M−He Dimers (M= Cu, Ag, Au): A Theoretical Investigation. *J. Chem. Phys.* **2008**, *129*, 204307.